Three-Dimensional Nano MHD Cross Fluid Flow: Effects of Convective Boundary Conditions, Thermal Radiation, and Heat Generation using similarity approach

Hemangini S Shukla[1], Pinal J Patel[2], Nikita V Thacker[3], Daxa M Diwan[4], Yamini M Parmar[5], Mahendra A Patel [6]

[1]Department of General, Government Engineering College, Gandhinagar -382028, India

hsshukla94@gmail.com

[2] Department of Computer Engineering, Government Engineering College, Modasa, India

pinal.patel@gecmodasa.ac.in

[3]Faculty of science, Shree Ram Krishna Institute of Computer Education and Applied Science, Surat, India

niki.thacker26@gmail.com

[4]Department of General, Government Engineering College, Bharuch, India

dm_diwan@yahoo.com

[5]Department of General, Government Engineering College, Gandhinagar-382028, India

ymp.maths@gmail.com

[6]Department of General, Government Engineering College, Modasa, India

dr.mahendraapatel@gmail.com

Abstract: This study focuses on the properties of a non-Newtonian three-dimensional cross nanofluid flow taking into account convective boundary conditions as well as the influence of thermophoresis and Brownian motion. Furthermore, the research analyse the effects of a thermal radiation, magnetic field, and heat generation. Similarity invariants are obtained from the governing equation of flow problem which are non-linear partial differential equations (PDEs). The non-linear PDEs are reduced into ordinary differential equations (ODEs), from which a similarity solution is obtained through the application of the established similarity invariants. The MATLAB bvp4c package's default solver for boundary value problems is employed to numerically solve obtained non-linear equations. A graphical analysis is conducted to show-case the effect of various parameters of fluid flow on temperature, concentration, and velocity profiles. Moreover, local skin friction coefficients, the rate of heat and mass transfer are tabulated and analysed.

Keywords: Cross fluid, Similarity solution, Nanofluid, MHD

Introduction:

Adding nanoparticles in the base fluid improves its thermal properties [1]. Nanofluids have various applications, including the cooling of microelectronics, thermal energy storage, solar power systems, and drug delivery mechanisms in medicine [2]. The non-Newtonian fluid models, including Powel-Eyring, Reiner-Philippoff, power law, Prandtl Eyring, and Sisko, play a crucial role in engineering and industrial applications [2,29,30,31,32,33]. However, these models are limited in their ability to analyze fluid behavior across varying shear rates. The fluid model namely Cross was created to investigate the behavior of fluids under both extremely low and high shear rates [3]. The Cross fluid model has proven effective in analyzing the behavior of blood, as well as 0.35% aqueous solutions of Xanthan gum ,0.40% aqueous solutions of polyacrylamide, and polymeric solutions. [20]

Magnetohydrodynamics (MHD) describes the interaction between magnetic fields and electrically conductive fluids. This phenomenon occurs in various environments, including the ionosphere, the sun, and power generation facilities. Additionally, non-Newtonian fluids are influenced by hydromagnetic effects. Non-Newtonian fluids and magnetism have significant role due to their diverse applications in both research and industry. These applications range from blood flow measurement techniques and turbo gear systems to the cooling of nuclear [4]. Consequently, numerous researchers have increasingly focused on examining the impacts of magnetic fields on heat transfer and mass transfer within the flow of nanofluids [5]. The analysis conducted by R. Codi et al. [4] for Maxwell mixed convection nanofluid around a vertical cone composed of porous material, with the effects of fluctuating diffusion and thermal conductivity Their findings shows that the presence of magnetic parameters causes a decrease in velocity.[4]

Literature Survey

A.M. Sedki [5] conducted a study of Cross fluid that includes nanoparticles and gyrotactic microorganisms over a horizontal cylinder situated within a porous material for bioconvective heat and mass transfer. This investigation took into account various factors such as thermophoresis, Brownian motion, magnetic fields, chemical reactions and thermal radiation. The findings indicated that the C_f (skin friction coefficient) increases with an increment in the magnetic parameter [5]. A research on the Casson fluid flow with nano particles across an inclined permeable stretching surface was carried out by Cui et al. [6], considering the impacts of heat generation, viscous dissipation, magnetic fields, thermal radiation and the characteristics of a porous medium, utilizing the Darcy–Forchheimer model through a local non-similarity approach. Their findings indicated that the frictional factor at the inclined stretching surface is enhanced by the influence of Lorentz forces and the porosity parameter [6]. Shah S. et al. [7] performed an investigation into the MHD flow of a Carreau fluid across a non-linear stretching or shrinking surface, while considering influences of chemical reactions and thermal radiation. They utilized similarity transformations to formulate a set of ODEs [7]. Ganesh et al. [8] performed an investigation on MHD Carreau nanofluid, by considering the effects of nonlinear type thermal radiation under slip conditions pertinent to heat and mass transfer boundaries. Their results indicated that rise in the radiation parameter within the boundary layer region results in an elevation of both the Nusselt (Nu_x) and Sherwood number (Sh_x) [8].

S. Nadeem et al. [9] examined the behavior of Maxwell MHD nanofluid over a vertically moving porous flat plate, by considering the effects of heat absorption, thermal radiation, and viscous dissipation. Their finding show that rise in the heat absorption coefficient results a decay in both the profile of temperature and the Sherwood number (Sh_x), and opposite behaviour Nusselt number (Nu_x) experiences an increase. Furthermore, Jyotshna, M., and Dhanalaxmi, V. [10] investigated the influence of convective conditions at boundary, thermal sources and sinks, thermal radiation, and activation energy on a porous stretched sheet. They employed a MHD Williamson nanofluid with GaN nanoparticles and ethylene glycol within a three-dimensional framework. They found that rising the heat source parameter results in a rise in the temperature profile, accompanied by a reduction in the concentration profile. Numerous researchers have examined the convective conditions at boundary of heat and mass in Newtonian and various non-Newtonian fluid models under diverse physical conditions, analyzing the impact of Biot numbers on the flow dynamics ([10],[11],[12]). The analysis of 2-Dimensional mixed convection cross fluid flow, incorporating convective boundary conditions and the effects of thermal radiation, was conducted by Mehwish Manzur et al. [18]. They analysed the same through the application of dimensionless variables to transform the system into ODEs.

The study of Cross axisymmetric fluid flow passing through a radially stretching sheet in cylindrical polar coordinates was conducted by M.Khan et al. [20]. They utilized similarity invariants to reformulate the governing equations into non-linear ODEs. T. Hayat et al. [19] considered the flow over a stretched surface in two dimensions for Cross fluid, transforming the equations of boundary layer into a non-dimensional form through appropriate transformations. M.I. Khan et al. [21] examined the 2-D flow of a Cross liquid that is incompressible and electrically conducting over a moving surface. They considered the influence of chemical reactions and activation energy on the nonlinear differential system. K. Masood et al. [22] analyzed two-dimensional flow over a linearly stretching sheet of Cross fluid by appropriate local similarity transformations. Additionally, A.M. Megahed and W. Abbas [23] explored the effect of chemical reactions and heat generation /absorption for cross fluid flow past a stratified stretching surface, incorporating thermal and solutal stratification boundary conditions.

We have derived similarity invariants for a 3-D Cross nanofluid model using Lie group theoretic method. Applying similarity invariants, we have obtained similarity equation which are ODEs.

Governing Equation of the Boundary Value Problem

Here we have worked on the three-dimensional Cross nano non-Newtonian type fluid model. The flow is incompressible, steady, laminar over a linearly stretching surface with the velocity $u_w = ax$ in X - direction and $v_w = by$ in Y-direction. In this case, the stretched sheet is subjected to magnetic field B applied uniformly oriented perpendicular to the surface. For the flow examination, the conditions of convective boundaries are taken into consideration. Heat generation/absorption impacts, as well as the impact of thermal radiation, are also considered in the heat transfer study. At an infinite distance from the sheet's surface, T_∞ and C_∞ are considered to be evenly dispersed temperature and concentration.

h_f = coefficient of heat transfer, h_s = coefficient of convective mass transfer, T_f = temperature of hot fluid, C_f = convective concentration of fluid

$$\frac{\partial u}{\partial x} + \frac{\partial v}{\partial y} + \frac{\partial w}{\partial z} = 0 \quad (1)$$

$$u\frac{\partial u}{\partial x} + v\frac{\partial u}{\partial y} + w\frac{\partial u}{\partial z} = \frac{\mu}{\rho}\frac{\partial}{\partial z}(\tau_1) - \frac{\sigma B^2}{\rho}u \quad (2)$$

$$u\frac{\partial v}{\partial x} + v\frac{\partial v}{\partial y} + w\frac{\partial v}{\partial z} = \frac{\mu}{\rho}\frac{\partial}{\partial z}(\tau_2) - \frac{\sigma B^2}{\rho}v \quad (3)$$

$$u\frac{\partial T}{\partial x} + v\frac{\partial T}{\partial y} + w\frac{\partial T}{\partial z} = \alpha_m\frac{\partial^2 T}{\partial z^2} + \tau\left[D_B\left(\frac{\partial T}{\partial z}\frac{\partial C}{\partial z}\right) + \frac{D_T}{T_\infty}\left(\frac{\partial T}{\partial z}\right)^2\right] + \frac{Q_0}{\rho c_p}(T - T_\infty) + \frac{1}{\rho c_p}\frac{\partial q_r}{\partial z} \quad (4)$$

$$u\frac{\partial C}{\partial x} + v\frac{\partial C}{\partial y} + w\frac{\partial C}{\partial z} = D_B\left(\frac{\partial^2 C}{\partial z^2}\right) + \frac{D_T}{T_\infty}\frac{\partial^2 T}{\partial z^2} \quad (5)$$

Boundary values for convective mode are given by:

$$u = u_w = ax, v = v_w = by, w = 0, -k\frac{\partial T}{\partial z} = h_f(T_f - T), -D_B\frac{\partial C}{\partial z} = h_s(C_f - C) \text{ at } z = 0$$

$$u = 0, v = 0, w = 0, T = T_\infty, C = C_\infty \text{ at } z = \infty \quad (6)$$

$\mu =$ *viscosity of the nanofluid*, $\rho =$ *density of the nanofluid*, and $\alpha_m =$ *thermal diffusivity of the nanofluid* , $k =$ *thermal conductivity*, ρc_p = *heat capacitance*

We have considered shearing stress and the rate of strain relationship in the following form.

$F\left(\tau_1, \frac{\partial u}{\partial z}\right) = 0$ and $G\left(\tau_2, \frac{\partial v}{\partial z}\right) = 0$ Where, Shear stress $\tau_1 = \frac{\frac{\partial u}{\partial z}}{1+\left(\Gamma\frac{\partial u}{\partial z}\right)^n}$ *and* $\tau_2 = \frac{\frac{\partial v}{\partial z}}{1+\left(\Gamma\frac{\partial v}{\partial z}\right)^n}$,

Γ = material time constant or consistency index, n= the power-law index, u =velocity of the fluid in the X direction, v =velocity of the fluid in the Y direction, w =velocity in the z direction, C = fluid concentration, T = fluid temperature, τ =heat capacitance ratio, ρ =fluid density, D_T = Coefficient of thermophoresis diffusion, D_B= Brownian diffusion coefficient, Q_0 = coefficient of internal heat generation, q_r = radiative heat flux, , α= thermal diffusivity, , σ = fluid electrical conductivity

$$q_r = \frac{-4\sigma^* {T_\infty}^3}{3k^*}\frac{\partial T^4}{\partial z},$$

Where k^* =absorption coefficient, σ^*= the Stefan–Boltzmann constant.

Here writing T^4 in terms of T_∞ by ignoring higher order terms as follows:

$$T^4 = T_\infty{}^4 + 4\,T_\infty{}^3 T - 4\,T_\infty{}^3 T_\infty$$

$$\frac{\partial q_r}{\partial z} = \frac{\partial}{\partial z}\left(\frac{-4\sigma^* T_\infty{}^3}{3k^*}\frac{\partial T^4}{\partial z}\right)$$

$$\frac{\partial q_r}{\partial z} = \frac{-16\sigma^* T_\infty{}^3}{3k^*}\frac{\partial^2 T}{\partial z^2} \tag{7}$$

Hence equation (4) is rewritten as

$$u\frac{\partial T}{\partial x} + v\frac{\partial T}{\partial y} + w\frac{\partial T}{\partial z} = \alpha_m \frac{\partial^2 T}{\partial z^2} + \tau\left[D_B\left(\frac{\partial T}{\partial z}\frac{\partial C}{\partial z}\right) + \frac{D_T}{T_\infty}\left(\frac{\partial T}{\partial z}\right)^2\right] + \frac{Q_0}{\rho c_p}(T - T_\infty) - \frac{1}{\rho c_p}\frac{16\sigma^* T_\infty{}^3}{3k^*}\frac{\partial^2 T}{\partial z^2} \tag{8}$$

By considering non-dimensional variable

$\theta = \frac{T - T_\infty}{T_f - T_\infty}$ and

$\phi = \frac{C - C_\infty}{C_f - C_\infty}$

(4), (5) and (6) number of equations are converted as follows:

$$u\frac{\partial \theta}{\partial x} + v\frac{\partial \theta}{\partial y} + w\frac{\partial \theta}{\partial z} = \alpha_m \frac{\partial^2 \theta}{\partial z^2} + \tau\left[(C_f - C_\infty)D_B\left(\frac{\partial \theta}{\partial z}\frac{\partial \phi}{\partial z}\right) + \frac{(T_f - T_\infty)D_T}{T_\infty}\left(\frac{\partial \theta}{\partial z}\right)^2\right] + \frac{Q_0}{\rho c_p}\theta - \frac{1}{\rho c_p}\frac{16\sigma^* T_\infty{}^3}{3k^*}\frac{\partial^2 \theta}{\partial z^2}$$
(9)

$$u\frac{\partial \phi}{\partial x} + v\frac{\partial \phi}{\partial y} + w\frac{\partial \phi}{\partial z} = D_B\left(\frac{\partial^2 \phi}{\partial z^2}\right) + \frac{T_f - T_\infty}{C_f - C_\infty}\frac{D_T}{T_\infty}\frac{\partial^2 \theta}{\partial z^2} \tag{10}$$

Invariance Analysis by Generalized Group Theoretic Method

Group theoretic method with two parameters have been applied. The three independent variable boundary value problem (BVP) is transformed into one independent variable problem. The two parameters group transformation in (c_1, c_2) is written as below.

$$G: \bar{s} = R^s(c_1, c_2) + \aleph^s(c_1, c_2)\, s \tag{11}$$

Where s refers u, v, w, $x, y, z, \theta, \phi, \tau_1, \tau_2$

$\aleph^S$ and R^S are real valued differentiable functions of (c_1, c_2)

Equations (1) to (5) of considered BVP with given boundary conditions remain invariant under the group of transformations defined in equation (11).

$$\frac{\partial \bar{u}}{\partial \bar{x}} + \frac{\partial \bar{v}}{\partial \bar{y}} + \frac{\partial \bar{w}}{\partial \bar{z}} = \mathbb{A}(c_1, c_2)\left(\frac{\partial u}{\partial x} + \frac{\partial v}{\partial y} + \frac{\partial w}{\partial z}\right) \tag{12}$$

$$\bar{u}\frac{\partial \bar{u}}{\partial \bar{x}} + \bar{v}\frac{\partial \bar{u}}{\partial \bar{y}} + \bar{w}\frac{\partial \bar{u}}{\partial \bar{z}} - \frac{\mu}{\rho}\frac{\partial \bar{\tau}_1}{\partial \bar{z}} + \frac{\sigma B^2}{\rho}\bar{u} =$$

$$\mathbb{B}(c_1, c_2)\left(u\frac{\partial u}{\partial x} + v\frac{\partial u}{\partial y} + w\frac{\partial u}{\partial z} - \frac{\mu}{\rho}\frac{\partial \tau_1}{\partial z} + \frac{\sigma B^2}{\rho}u\right) + \mathbb{C}(c_1, c_2) \tag{13}$$

$$\bar{u}\frac{\partial \bar{v}}{\partial \bar{x}} + \bar{v}\frac{\partial \bar{v}}{\partial \bar{y}} + \bar{w}\frac{\partial \bar{v}}{\partial \bar{z}} - \frac{\mu}{\rho}\frac{\partial \bar{\tau}_2}{\partial \bar{z}} + \frac{\sigma B^2}{\rho}\bar{v} =$$

$$\mathbb{D}(c_1,c_2)\ (u\frac{\partial v}{\partial x}+v\frac{\partial v}{\partial y}+w\frac{\partial v}{\partial z}-\frac{\mu}{\rho}\frac{\partial \tau_2}{\partial z}+\frac{\sigma B^2}{\rho}v)+\mathbb{E}(c_1,c_2) \tag{14}$$

$$\bar{u}\frac{\partial \bar{\theta}}{\partial \bar{x}}+\bar{v}\frac{\partial \bar{\theta}}{\partial \bar{y}}+\bar{w}\frac{\partial \bar{\theta}}{\partial \bar{z}}-\alpha_m\frac{\partial^2\bar{\theta}}{\partial \bar{z}^2}-\tau[(C_f-C_\infty)D_B\left(\frac{\partial \bar{\theta}}{\partial \bar{z}}\frac{\partial \bar{C}}{\partial \bar{z}}\right)+\frac{(T_f-T_\infty)D_T}{T_\infty}\left(\frac{\partial \bar{\theta}}{\partial \bar{z}}\right)^2-\frac{Q_0}{\rho c_p}\bar{\theta}+\frac{(T_f-T_\infty)}{\rho c_p}\frac{16\sigma^* T_\infty{}^3}{3k^*}\frac{\partial^2\bar{\theta}}{\partial \bar{z}^2}=$$

$$\mathbb{F}(c_1,c_2)(u\frac{\partial \theta}{\partial x}+v\frac{\partial \theta}{\partial y}+w\frac{\partial \theta}{\partial z}-\alpha_m\frac{\partial^2\theta}{\partial z^2}+\tau\left[(C_f-C_\infty)D_B\left(\frac{\partial \theta}{\partial z}\frac{\partial \phi}{\partial z}\right)+\frac{(T_f-T_\infty)D_T}{T_\infty}\left(\frac{\partial \theta}{\partial z}\right)^2\right]+\frac{Q_0}{\rho c_p}\theta+\frac{(T_f-T_\infty)}{\rho c_p}\frac{16\sigma^* T_\infty{}^3}{3k^*}\frac{\partial^2\theta}{\partial z^2})+\mathbb{G}(c_1,c_2) \tag{15}$$

$$\bar{u}\frac{\partial \bar{\phi}}{\partial \bar{x}}+\bar{v}\frac{\partial \bar{\phi}}{\partial \bar{y}}+\bar{w}\frac{\partial \bar{\phi}}{\partial \bar{z}}-D_B\left(\frac{\partial^2\bar{\phi}}{\partial \bar{z}^2}\right)-\frac{T_f-T_\infty}{C_f-C_\infty}\frac{D_T}{T_\infty}\frac{\partial^2\bar{\theta}}{\partial \bar{z}^2}=\mathbb{H}(c_1,c_2)\ u\left(\frac{\partial \phi}{\partial x}+v\frac{\partial \phi}{\partial y}+w\frac{\partial \phi}{\partial z}-D_B\left(\frac{\partial^2\phi}{\partial z^2}\right)-\frac{T_f-T_\infty}{C_f-C_\infty}\frac{D_T}{T_\infty}\frac{\partial^2\theta}{\partial z^2}\right)+\mathbb{I}(c_1,c_2) \tag{16}$$

$$F\left(\bar{\tau_1},\frac{\partial \bar{u}}{\partial \bar{z}}\right)=\mathbb{J}(c_1,c_2)F\left(\tau_1,\frac{\partial u}{\partial z}\right)+\mathbb{K}((c_1,c_2) \tag{17}$$

$$G\left(\bar{\tau_2},\frac{\partial \bar{v}}{\partial \bar{z}}\right)=\mathbb{L}(c_1,c_2)G\left(\tau_2,\frac{\partial v}{\partial z}\right)+\mathbb{M}(c_1,c_2) \tag{18}$$

The invariance of above equations implies that

$$\mathbb{C}(c_1,c_2)\ =\mathbb{E}(c_1,c_2)=\mathbb{G}(c_1,c_2)==\mathbb{I}(c_1,c_2)=\mathbb{K}((c_1,c_2)\ =\ \mathbb{M}(c_1,c_2)=\ 0$$

This is satisfied if we take $R^u=R^v=R^w=R^\theta=R^\phi=R^{\tau_1}=R^{\tau_2}=0$

$$\mathbb{A}(c_1,c_2)=\frac{\aleph^u}{\aleph^x}=\frac{\aleph^v}{\aleph^y}=\frac{\aleph^w}{\aleph^z} \tag{19}$$

$$\mathbb{B}(c_1,c_2)=\frac{(\aleph^u)^2}{\aleph^x}=\frac{\aleph^u\aleph^v}{\aleph^y}=\frac{\aleph^u\aleph^w}{\aleph^z}=\frac{\aleph^{\tau_1}}{\aleph^z}=\aleph^u \tag{20}$$

$$\mathbb{D}(c_1,c_2)=\frac{(\aleph^v)^2}{\aleph^y}=\frac{\aleph^u\aleph^v}{\aleph^x}=\frac{\aleph^v\aleph^w}{\aleph^z}=\frac{\aleph^{\tau_2}}{\aleph^z}=\aleph^v \tag{21}$$

$$\mathbb{F}(c_1,c_2)=\frac{\aleph^u\aleph^\theta}{\aleph^x}=\frac{\aleph^v\aleph^\theta}{\aleph^y}=\frac{\aleph^w\aleph^\theta}{\aleph^z}=\frac{\aleph^\theta}{(\aleph^z)^2}=\frac{\aleph^\theta\aleph^C}{(\aleph^z)^2}=(\frac{\aleph^\theta}{\aleph^z})^2 \tag{22}$$

$$\mathbb{H}(c_1,c_2)=\frac{\aleph^u\aleph^\phi}{\aleph^x}=\frac{\aleph^v\aleph^\phi}{\aleph^y}=\frac{\aleph^w\aleph^\phi}{\aleph^z}=\frac{\aleph^\phi}{(\aleph^z)^2}=(\frac{\aleph^\theta}{\aleph^z})^2$$

$$\mathbb{J}(c_1,c_2)=\aleph^{\tau_1}=1 \tag{23}$$

$$\mathbb{L}(c_1,c_2)=\aleph^{\tau_2}=1$$

So, from equation (19) to (23) with boundary conditions (BCs) in (6), derived following relations between functions of two parameters.

$$\aleph^u=\aleph^x,\aleph^v=\aleph^y,\aleph^w=\aleph^z=\aleph^\phi=\aleph^\theta=\aleph^{\tau_1}=\aleph^{\tau_2}=1,$$

$$R^u=R^x=R^v=R^y=R^w=R^z=R^\theta=R^\phi=R^{\tau_1}=R^{\tau_2}=0 \tag{24}$$

The group transformation of two-parameter is derived in following form.

$$G:\begin{cases}\bar{x}=\aleph^{x}x\\ \bar{u}=\aleph^{x}u\\ \bar{y}=\aleph^{y}y\\ \bar{v}=\aleph^{y}v\\ \bar{w}=w\\ \bar{z}=z\\ \bar{\theta}=\theta\\ \bar{\phi}=\phi\\ \bar{\tau_1}=\tau_1\\ \bar{\tau_2}=\tau_2\end{cases}$$

Using above similarity variables, we derived following equations by transforming governing equations (1) to (6) with conditions at boundary.

$$g_1+cg_2-g_3{}'=0$$

$$[1+(1-n)We_1{}^n(g_1{}')^n]g_1''-[1+We_1{}^n(g_1{}')^n\,]^2[\,(g_1)^2-g_3g_1'+Mg_1]=0 \tag{25}$$

$$[1+(1-n)We_2{}^n(g_2{}')^n]g_2''-[1+We_2{}^n(g_2{}')^n\,]^2[\,c(g_2)^2-g_3g_2'+Mg_2]=0 \tag{26}$$

$$\frac{1}{pr}(1+R_d)g_4''+\ g_4'+\lambda_1g_4+N_b\,g_4'\,g_5'+N_t\,(g_4')^2+g_3\,g_4'=0 \tag{27}$$

$$g_5''+\frac{N_t}{N_b}\,g_4''+Sc\,g_5'\,g_3=0 \tag{28}$$

with boundary conditions:

At $\eta=0, g_1=1, g_2=c, g_3=0,\ g_4'=-\frac{Bi_1}{\varepsilon_4}(1-g_4),\ g_5'=-Bi_2(1-g_5),$

$$\text{At }\ \eta=\infty, g_1=g_2=g_3=g_4=g_5=0 \tag{29}$$

$Re_x=\frac{u_wx}{\vartheta_f}, Re_y=\frac{v_wy}{\vartheta_f},$

Where, $We_1=\Gamma ax\sqrt{\frac{a}{\vartheta_f}}=\Gamma a(Re_x)^{\frac{1}{2}}, We_2=\Gamma by\sqrt{\frac{a}{\vartheta_f}}=$ $\Gamma a\sqrt{c}(Re_y)^{\frac{1}{2}}$ is the local Weissenberg number, $M=\frac{\sigma B^2}{a\rho_f}, N_b=\ \tau D_B\frac{(C_f-C_\infty)}{\vartheta_f}, N_t=$ $\tau\frac{D_T}{T_\infty}\frac{(T_f-T_\infty)}{\vartheta_f}, \frac{Q_0}{a\rho c_f}=\lambda_1, pr=\frac{\vartheta_f}{\alpha}=\frac{(\mu c_p)_f}{k_f}, R_d=\frac{-16\sigma T_\infty{}^3}{3kk^*}, Sc=\frac{\vartheta_f}{D_B},\quad Bi_1=\frac{h_f}{k_f}\sqrt{\frac{\vartheta_f}{a}}, Bi_2=\frac{h_s}{D_B}\sqrt{\frac{\vartheta_f}{a}},\ \frac{b}{a}=$ $c=alpha$

To reduce one equation, take $g_1=G_1', g_2=G_2'$

$$g_1+cg_2-g_3{}'=0\Rightarrow G_1+cG_2=g_3$$

$$[1+(1-n)We_1{}^n(g_1{}')^n]g_1''-[1+We_1{}^n(g_1{}')^n\,]^2[\,(g_1)^2-\ g_3g_1'+Mg_1]=0 \tag{30}$$

$$\Rightarrow$$

$$[1+(1-n)We_1{}^n(G_1'')^n]G_1'''-[1+We_1{}^n(G_1{}'')^n\,]^2[\,(G_1{}')^2-(G_1+cG_2)G_1{}''+MG_1']=0 \tag{31}$$

$$[1+(1-n)We_2{}^n(g_2{}')^n]g_2''-[1+We_2{}^n(g_2{}')^n\,]^2[\,c(g_2)^2-g_3g_2'+Mg_2]=0 \tag{32}$$

$$\Rightarrow$$

$$[1+(1-n)We_1{}^n(G_2'')^n]G_2'''-[1+We_1{}^n(G_2{}'')^n\,]^2[c\,(G_2{}')^2-(G_1+cG_2)G_2{}''+MG_2']=0 \tag{33}$$

$$(1+R_d)\frac{1}{Pr}g_4''+\ g_4'+\lambda_1g_4+N_b\,g_4'\,g_5'+N_t\,(g_4')^2+(G_1+cG_2)\,g_4'=0 \tag{34}$$

$$g_5'' + \frac{N_t}{N_b}\, g_4'' + Sc\, g_5' \,(G_1 + cG_2) = 0 \quad (35)$$

$$[1 + (1-n)We_1{}^n (G_1'')^n]G_1''' - [1 + We_1{}^n (G_1'')^n\,]^2[\,(G_1')^2 - (G_1 + cG_2)G_1'' + MG_1'] = 0 \quad (36)$$

$$[1 + (1-n)We_1{}^n (G_2'')^n]G_2''' - [1 + We_1{}^n (G_2'')^n\,]^2[c\,(G_2')^2 - (G_1 + cG_2)G_2'' + MG_2'] = 0 \quad (37)$$

$$\frac{1}{pr}(1 + R_d)g_4'' + \; g_4' + \lambda_1 g_4 + N_b\, g_4'\, g_5' + N_t\,(g_4')^2 + \; g_4'(G_1 + cG_2) = 0 \quad (38)$$

$$g_5'' + \frac{N_t}{N_b}\, g_4'' + Sc\, g_5'(G_1 + cG_2) \; = 0 \quad (39)$$

$$\frac{1}{2}(Re_x)^{\frac{1}{2}}C_{fx} = \frac{G_1''(0)}{1 + We_1{}^n\left(G_1''(0)\right)^n}, \frac{1}{2}(Re_y)^{\frac{1}{2}}C_{fy} = \frac{G_2''(0)}{1 + We_2{}^n\left(G_2''(0)\right)^n}, where Re_x = \frac{u_w x}{\vartheta_f}, Re_y = \frac{v_w y}{\vartheta_f} \quad (40)$$

$$(Re)^{-\frac{1}{2}}Nu_x = -g_4'(0) \quad (41)$$

$$(Re)^{-\frac{1}{2}}Sh_x = -g_5'(0) \quad (42)$$

with boundary conditions:

$$At\, \eta = 0, G_1' = 1, G_2' = c, G_1 + cG_2 = 0, \; g_4' = -Bi_1(1 - g_4), \; g_5' = -Bi_2(1 - g_5),$$

$$At \;\; \eta = \infty, G_1' = G_2' = G_1 + cG_2 = g_4 = g_5 = 0 \quad (43)$$

Numerical solution:

We must transform the aforementioned system of equations in order to use Bvp4c, into a system of differential equations of first order.

Take $\boldsymbol{y_1, y_2, y_3}$ as $\boldsymbol{G_1, G_1', G_1''}$ and $\boldsymbol{y_4, y_5, y_6}$ as $\boldsymbol{G_2, G_2', G_2''}$ respectively. $\boldsymbol{y_7, y_8}$, $\boldsymbol{y_9, y_{10}}$ as $\boldsymbol{g_4, g_4', g_5, g_5'}$ respectively.

$$y'_1 = y_2 \quad (44)$$

$$y'_2 = y_3 \quad (45)$$

$$y'_3 = \frac{[1 + We_1{}^n (y_3)^n\,]^2[\,\varepsilon_1 c (y_2)^2 - \varepsilon_1 (y_1 + c y_4) y_3 + M y_2]}{\varepsilon_2[1 + (1-n)We_1{}^n (y_3\,)^n]} \quad (46)$$

$$y'_4 = y_5 \quad (47)$$

$$y'_5 = y_6 \quad (48)$$

$$y'_6 = \frac{[1 + We_2{}^n (y_6)^n\,]^2[\,\varepsilon_1 c (y_5)^2 - \varepsilon_1 (y_1 + c y_4) y_6 + M y_5]}{\varepsilon_2[1 + (1-n)We_2{}^n (y_6\,)^n]} \quad (49)$$

$$y'_7 = y_8 \quad (50)$$

$$y'_8 = \frac{-pr(\,g_4' + \lambda_1 g_4 + N_b\, g_4'\, g_5' + N_t\,(g_4')^2}{(1 + R_d)} \;\; = \frac{-pr(y_8 + \lambda_1 y_7 + N_b y_8 y_{10} + N_t (y8)^2 + y_8(y_1 + c y_4)\,)}{(1 + R_d)} \quad (51)$$

$$y'_9 = y_{10} \quad (52)$$

$$y'_{10} = -\frac{N_t}{N_b}\, g_4'' - Sc\, g_5'\,(G_1 + cG_2) = -\frac{N_t}{N_b} y'_8 - Sc(y_1 + c y_4) y_{10} \quad (53)$$

with boundary conditions

$$\text{At } \eta = 0, [y_2 = 1, y_5 = c, y_1 + c y_4 = 0, y_8 = -\frac{Bi_1}{\varepsilon_4}(1 - y_7(0)), y_{10} = -Bi_2(1 - y_9(0))]$$

$$\text{At } \;\; \eta = \infty, [y_2 = y_5 = y_1 + c y_4 = y_7 = y_9 = 0] \quad (54)$$

Result and Discussion

We had analysed heat transfer for different parameters like Thermophoresis parameter (N_t), Prandtl number (pr), Brownian motion parameter (N_b), radiation parameter (R_d) and heat generation parameter (λ_1). Figures 1 to 5 shows that how various parameters affect the temperature profile.

Figure 1 indicates the Prandtl number and the thermal profile relationship. Figure shows that as increasing (pr), temperature profile decreases. Lower Prandtl number (pr) values correspond to higher thermal diffusivity. So, more heat would spread through such fluids, resulting in higher temperature. Theoretically, the Prandtl number (pr) and thermal diffusivity are in inverse proportion, leading to inclination in the thermal profile. Also, figure 1 shows that temperature profile higher for $n < 1$ then $n > 1$.

The impact of the thermophoresis parameter (N_t) on temperature is illustrated in Figure 2. The thermophoresis parameter affects temperature by influencing how particles flow across a fluid medium. A higher thermophoresis parameter signifies a stronger thermophoretic force. In physical terms, N_t represents the temperature difference in the cross nanofluid, defined as the difference between the heated fluid temperature behind the sheet and the liquid temperature at an infinite distance. As a result, increasing the N_t values results in a greater temperature disparity between the infinite region and the surface, thereby contributing to an augmentation in the temperature of the cross nanofluid. Figure 2 shows increase in temperature profile as raising N_t in all cases for n =1, n less than and n greater than 1.

Figure 3 demonstrates the outcome of heat generation/absorption parameter (λ_1) on temperature. The heat transfer phenomenon is enhanced by the internal heat generation/absorption parameter. Figure 3 shows an increase in (λ_1) heat generation/absorption parameter temperature profile rises.

Figure 4 indicates the influence of the R_d on temperature profile. Due to the increment in radiation parameter heat transfer escalates, and enhances thermal profile. Same phenomenon observed for all values of n. Figure 5 indicates impact of $\mathrm{N_t}$ on Concentration profile for Shear thinning, Newtonian and Shear thickening fluid. From a theoretical perspective, a greater thermophoresis parameter indicates a stronger thermophoretic force. This stronger force causes a significant movement of fluid particles. The fluid particles move from hot surface towards the cooler regions. Due to this movement concentration of nanoparticles increased in those areas. So, in figure 5 we observed increased concentration boundary layer as values of $\mathrm{N_t}$ raises in all three fluid types.

Impact of $\mathrm{N_b}$ on Concentration profile for Newtonian (n =1), shear thinning (n less than 1) and shear thickening (n greater than 1) fluid is depicted in Figure 6. Physically, Brownian motion leads particles to move against the concentration gradient, to get a more homogeneous nanofluid. Because of this motion of nanoparticles, the concentration profile decreases. Similar trend observed in figure 6 for all different values of n.

The rise in the Sc (Schmidt number) leads to reduced Brownian motion, resulting in a decrease in nanoparticle concentrations. Figure 7 shows, a higher Schmidt number decline in nanoparticle concentration due to greater molecular diffusivity.

Figure 8 indicates the fluctuations of N_t (Nusselt number) for various values of Bi_1, Bi_2 (thermal biot numbers) and radiation parameter. The increased convective heating reduces the rate of heat transfer from the stretched sheet. The convective heat transfer mode means to heat or cool the sheet's surface by a hot fluid with temperature T_f. Convective heating is the reason for the rise in fluid temperature.

The fluctuations in $(Re)^{-\frac{1}{2}}Sh_x$ (Sherwood number) for radiation parameter and for different values of (Bi_1, Bi_2) biot numbers is shown in figure 9. This figure makes it clear that rise in biot number is the reason to Sherwood number grows. It indicates that as biot number grows, the mass transfer rate develops.

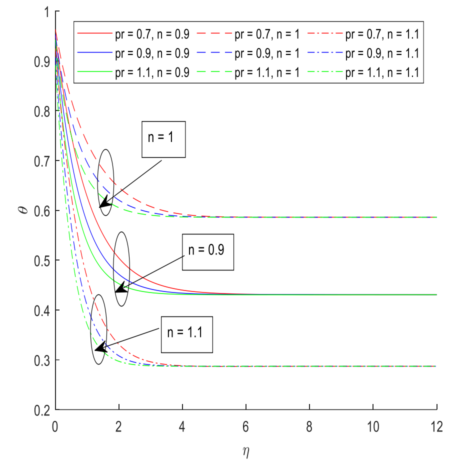

Figure 1 Temperature(θ) profile for Shear thinning, Newtonian(n =1), and Shear thickening fluid for different pr

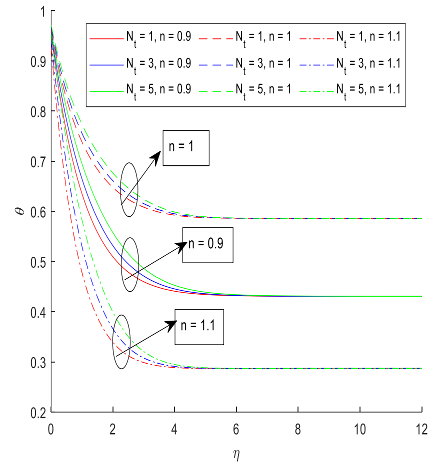

Figure 2 Temperature(θ) profile for Shear thinning, Newtonian(n =1), and Shear thickening fluid for different N_t

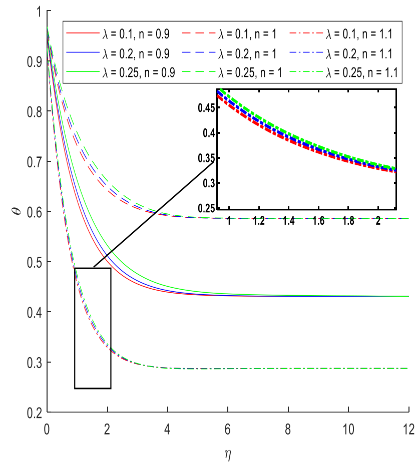

Figure 3 Temperature(θ) profile for Shear thinning, Newtonian(n =1), and Shear thickening fluid for different λ

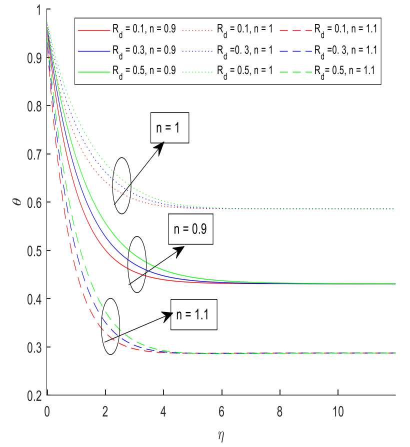

Figure 4 Temperature(θ) profile for Shear thinning, Newtonian(n =1), and Shear thickening fluid for different R_d

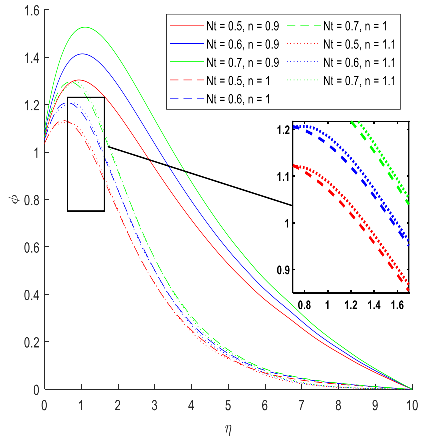

Figure 5 Concentration profile for Shear thickening, Newtonian(n =1), and Shear thinning fluid for different N_t

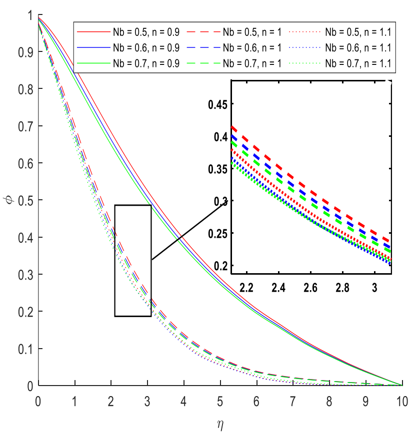

Figure 6 Concentration profile for Shear thickening, Newtonian(n =1), and Shear thinning fluid for different N_b

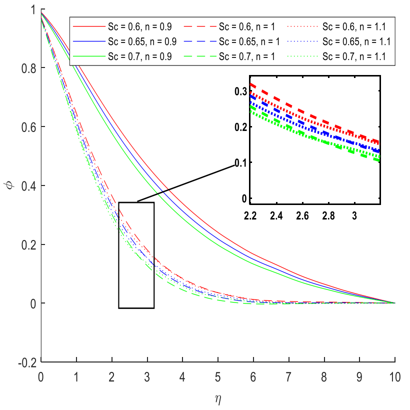

Figure 7 Concentration profile for Shear thinning, Newtonian(n =1), Shear thickening fluid for different Sc

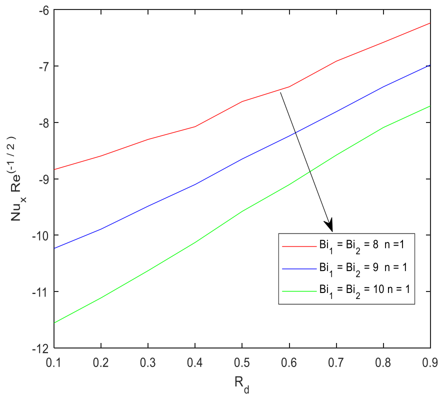

Figure 8 Impact on Nusselt number(Nu_x) for Newtonian fluid(n =1), Bi_1 and Bi_2 and for different R_d

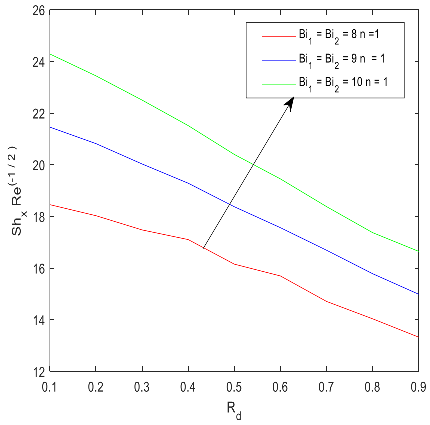

Figure 9 Impact of Bi_1 and Bi_2 and R_d on Sherwood number for Newtonian fluid(n =1)

Numerical Solution:

Table 1 and Table 2 shows numerical data of (Sh_x) Sherwood number, (Nu_x) Nusselt number and skin friction coefficients (C_{fx}, C_{fy}) for various physical parameters. Impact of (c) stretching ratio parameter,

(pr) Prandtl number, (N_t) Thermophoresis parameter, (N_b) parameter of Brownian motion and (Sc) Schmidt number on both (Sh_x) Sherwood number and (Nu_x) Nusselt number is presented in Table 1. As (Sc) Schmidt number grows, (Sh_x) Sherwood number and (Nu_x) Nusselt number declines. Same trend observed for (N_t) Thermophoresis parameter. Sherwood number accelerates and Nusselt number decreases as (N_b) Brownian motion parameter, (c) stretching ratio parameter and (pr) Prandtl number increases.

Effects of magnetic parameter(M), Weissenberg number(We_1, We_2), stretching ratio parameter (c) and the power-law index (n) on skin friction coefficients (C_{fx}, C_{fy}) is depicted in Table 2. Growing (M) magnetic parameter, (C_{fx}) X-directional skin friction coefficient is growing whereas reverse impact on $\left(C_{fy}\right)$ Y-directional skin friction coefficient. As local Weissenberg number (We_1) accelerates X-directional skin coefficient(C_{fx}) whereas declines Y-directional skin friction coefficient(C_{fy}). Reverse trends observed for Weissenberg number (We_2). X-directional skin coefficient (C_{fx}) declines and Y-directional skin friction coefficient (C_{fy}) grows for increase in stretching ratio parameter (c) and power-law index(n).

Table 1:

C	pr	N_t	N_b	Sc	Sh_x	Nu_x
0.9	0.7	0.5	0.1	0.1	-3.70057517286095	0.722776517903128
0.9	0.7	0.5	0.1	0.2	-3.95082702597790	0.721931209945843
0.9	0.7	0.5	0.1	0.3	-4.16571065016962	0.717464519154662
0.9	0.7	0.5	0.1	0.4	-4.40128529043976	0.714922709671519
0.9	0.7	0.5	0.2	0.4	-3.41176185307158	0.708635291168439
0.9	0.7	0.5	0.3	0.4	-3.07528510011997	0.701842408808120
0.9	0.7	0.5	0.4	0.4	-2.90811657867256	0.694365854994777
0.9	0.7	0.6	0.4	0.4	-2.99007584203396	0.691794363956845
0.9	0.7	0.7	0.4	0.4	-3.06551727954635	0.689259936463397
0.9	0.7	0.8	0.4	0.4	-3.14156483818735	0.686840571102522
0.9	1	0.8	0.4	0.4	-2.63424577647820	0.613571074796583
0.9	1.5	0.8	0.4	0.4	-0.74881679515678	-0.000794467636910
0.9	2	0.8	0.4	0.4	1.93911540196176	-1.053993193841240
1.1	0.7	0.8	0.4	0.4	-3.62575529832887	0.688784250586004
1.3	0.7	0.8	0.4	0.4	-0.77617455709581	0.323046651755941
1.5	0.7	0.8	0.4	0.4	1.97501683547182	-0.177429481047915

Table 2:

M	We_1	We_2	C	n	C_{fx}	C_{fy}
0.1	2.2	2.2	1	1	0.342437275092393	0.666973956893875
0.2	2.2	2.2	1	1	0.453571908128068	-0.106328487627370
0.3	2.2	2.2	1	1	0.453751787015479	-0.108580752332336
0.3	2.4	2.2	1	1	0.506602412167393	-0.096127508782605
0.3	2.5	2.2	1	1	0.399990376932584	-0.103759801383984
0.3	2.6	2.2	1	1	0.384524176624877	0.446877991818451
0.3	2.2	2.4	0.9	1	0.455112664259661	-0.052018790488570
0.3	2.2	2.5	0.9	1	0.464351781500088	-0.061529111378182
0.3	2.2	2.6	0.9	1	0.482445626153410	-0.100054391617870
0.3	2.2	2.2	1.7	1	0.455222887378393	-0.081019079799131
0.3	2.2	2.2	1.8	1	0.454855007015849	-0.054029912778095
0.3	2.2	2.2	1.9	1	0.454258443014128	-0.043476486217571

0.3	2.2	2.2	1	0.9	0.618713703697608	-0.130312288899883
0.3	2.2	2.2	1	1	0.453751787015479	-0.108580752332336
0.3	2.2	2.2	1	1.1	0.249935194837912	-0.097045409225205

Conclusion:

- Temperature of cross fluid is elevated as increasing value of N_t.
- The increasing values of pr, λ, Rd decreases cross fluid temperature.
- The concentration profile accelerates as increasing N_t whereas opposite impact of $N_b$and Sc.
- The increasing values of Biot numbers resulted in the elevation of the Sherwood number whereas opposite effect on Nusselt number.
- Skin friction coefficient (C_{fx}) in x-direction decreases as value of power-low index increases.We_1 increases then C_{fx} decreases.and reverse impact of We_2.
- The temperature profile of a Newtonian fluid is higher compared to both shear-thinning$(n < 1)$ and shear-thickening$(n > 1)$ fluids, indicating that Newtonian fluids retain more heat due to their consistent viscosity, whereas non-Newtonian fluids exhibit varying thermal conductivity and flow resistance, affecting heat distribution.
- The concentration profile of a shear-thinning fluid$(n < 1)$ is higher than that of Newtonian$(n = 1)$ and shear-thickening $(n > 1)$ fluids, suggesting that reduced viscosity at higher shear rates enhances mass transport and diffusion, leading to a more uniform distribution of solute particles.

References

[1] Choi, S.U.S., 1995. Enhancing Thermal Conductivity of Fluids with Nanoparticles. In: Developments and Applications of Non-Newtonian Flows, Siginer, D.A. any d H.P. Wang (Eds.). American Society of Mechanical Engineers, New York, pp: 99-105.

[2] Shukla, Hemangini, Surati, Hema, Timol, Munir 2020/05/22, pp. 203- 212 Similarity Analysis of MHD Three Dimensional Nanofluid Flow for Non-Newtonian Power-Law Model over Linearly Stretching Sheet with Convective Boundary Conditions, Vol. 38, March, 2020, 10.18280/ijht.380122, International Journal of Heat and Technology

[3] Cross, M.M. (1965). Rheology of non-Newtonian fluids: A new flow equation for pseudoplastic systems. J. Colloid Sci., 20(5): 417-437.

[4] Raghunath Kodi, Charankumar Ganteda, Abhishek Dasore, M. Logesh Kumar, G. Laxmaiah, Mohd Abul Hasan, Saiful Islam, Abdul Razak ,Influence of MHD mixed convection flow for maxwell nanofluid through a vertical cone with porous material in the existence of variable heat conductivity and diffusion,Case Studies in Thermal Engineering,Volume 44,2023,102875,ISSN 2214-157X,

[5] Ahmed M. Sedki,Computational analysis of MHD Cross nanofluid containing gyrotactic microorganisms over a permeable horizontal cylinder through a porous medium in presence of thermal radiation and chemical reaction,Partial Differential Equations in Applied Mathematics,Volume 7,2023,100508,ISSN 2666-8181,https://doi.org/10.1016/j.padiff.2023.100508.

[6] Cui, J.; Jan, A.; Farooq, U.; Hussain, M.; Khan, W.A. Thermal Analysis of Radiative Darcy– Forchheimer Nanofluid Flow Across an Inclined Stretching Surface. Nanomaterials 2022, 12, 4291. https:// doi.org/10.3390/nano12234291

[7] Shah, S.A.G.A., Hassan, A., Karamti, H. *et al.* Effect of thermal radiation on convective heat transfer in MHD boundary layer Carreau fluid with chemical reaction. *Sci Rep* 13, 4117 (2023). https://doi.org/10.1038/s41598-023-31151-4

[8] Ganesh Kumar, K., Ramesh, G.K., Gireesha, B.J. and Rashad, A.M.. "On stretched magnetic flow of Carreau nanofluid with slip effects and nonlinear thermal radiation" *Nonlinear Engineering*, vol. 8, no. 1, 2019, pp. 340-349. https://doi.org/10.1515/nleng-2017-0120

[9] Sohail Nadeem, Salman Akhtar, Nadeem Abbas, Heat transfer of Maxwell base fluid flow of nanomaterial with MHD over a vertical moving surface, Volume 59, Issue 3,2020, Pages 1847-1856, ISSN 1110-0168, https://doi.org/10.1016/j.aej.2020.05.008.

[10] Jyotshna, M. ., & Dhanalaxmi, V. (2022). Impact of Activation Energy and Heat Source/Sink on 3D Flow of Williamson Nanofluid with GaN Nanoparticles over A Stretching Sheet. *European Journal of Mathematics and Statistics*, *3*(5), 16–29. https://doi.org/10.24018/ejmath.2022.3.5.133

[11] Khan AS, Nie Y, Shah Z, Dawar A, Khan W, Islam S. Three-Dimensional Nanofluid Flow with Heat and Mass Transfer Analysis over a Linear Stretching Surface with Convective Boundary Conditions. *Applied Sciences*. 2018; 8(11):2244. https://doi.org/10.3390/app8112244

[12] Gamsha, Abdullahi & Hussaini, Abubakar. (2023). Modified Mathematical Model on the Study of Convective MHD Nanofluid Flow with Heat Generation/Absorption along with Thermophoresis and Brownian Motion on Boundary Layer Flow over a Linearly Stretching Sheet. Journal of Modern Mathematics and Statistics. 15. 39- 46.

[13] Shukla, H., Patel, J., Surati, H.C., Patel, M., Timol, M.G. (2017). Similarity solution of forced convection flow of Powell-Eyring & Prandtl-Eyring fluids by grouptheoretic method. Mathematical Journal of Interdisciplinary Sciences, 5(2): 151-165. https://doi.org/10.15415/mjis.2017.52012

[14] Shukla, H., Surati, H.C., Timol, M.G. (2018). Similarity analysis of three dimensional nanofluid flow by deductive group theoretic method. Applications and Applied Mathematics-An International Journal, 13(2): 1260-1272.

[15] Surati, H. C., Shukla, H., Timol, M.G. (2016). On the Transformation of Non-Newtonian Boundary value problem to Initial value problem. Int. J. of Engg. Sc. Invention Research & Development; Vol. III, Issue III, pp.180-189.

[16] Finite Difference Method on Third-order Non-linear Differential Equation: Magneto Hydrodynamic Flow of Sisko Fluid. Jayshri Patel, Hemangini Shukla, Manisha Patel, Hema C. Surati and M.G. Timol, INDIAN JOURNAL OF INDUSTRIAL AND APPLIED MATHEMATICS Vol. 8, No. 2, July–December 2017, pp. 191–200, DOI: 10.5958/1945-919X.2017.00017.2

[17] Similarity Analysis of MHD Three Dimensional Nanofluid Flow for Non-Newtonian Power-Law Model over Linearly Stretching Sheet with Convective Boundary Conditions Hemangini S. Shukla, Hema C. Surati, Munir G. Timol, International Journal of Heat and Technology Vol. 38, No. 1, March, 2020, pp. 203-212, https://doi.org/10.18280/ijht.380122

[18] Mehwish Manzur, Masood Khan, Masood ur Rahman, Mixed convection heat transfer to cross fluid with thermal radiation: Effects of buoyancy assisting and opposing flows, International Journal of Mechanical Sciences,Volumes 138–139,2018,Pages 515-523,ISSN 0020-7403, https://doi.org/10.1016/j.ijmecsci.2018.02.010**.**

[19] T. Hayat, M. Ijaz Khan, M. Tamoor, M. Waqas, A. Alsaedi, Numerical simulation of heat transfer in MHD stagnation point flow of Cross fluid model towards a stretched surface, Results in Physics, Volume 7, 2017,Pages 1824-1827, ISSN 2211-3797, https://doi.org/10.1016/j.rinp.2017.05.022**.**

[20] Masood Khan, Mehwish Manzur, Masood ur Rahman, On axisymmetric flow and heat transfer of Cross fluid over a radially stretching sheet,Results in Physics, Volume 7,2017,Pages 3767-3772,ISSN 2211-3797,https://doi.org/10.1016/j.rinp.2017.08.039.

[21] M. Ijaz Khan, M. Waqas, T. Hayat and A. Al-saedi, Magneto-hydrodynamical numerical simulation of heat transfer in MHD stagnation point flow of Cross fluid model towards a stretched surface, Physics and Chemistry of Liquids,Vol.56,No.5,pages = {584--595},2018, https://doi.org/10.1080/00319104.2017.1367791

[22] Boundary-layer flow and heat transfer of cross fluid over a stretching sheet,Khan Masood,Manzur Mehwish,Rahman Masood ur, Thermal Science,2019,Vol. – 23,Issue – 1,PP – 307-318

[23] Ahmed M. Megahed, W. Abbas,Non-Newtonian Cross fluid flow through a porous medium with regard to the effect of chemical reaction and thermal stratification phenomenon, Case Studies in Thermal Engineering,Volume 29,2022,https://doi.org/10.1016/j.csite.2021.101715